### **Device**



### **Perspective**

# 2D transition metal dichalcogenides for energy-efficient two-terminal optoelectronic synaptic devices

Roshni Satheesh Babu<sup>1</sup> and Dimitra G. Georgiadou<sup>1,2,\*</sup>

- <sup>1</sup>School of Electronics and Computer Science, University of Southampton, Southampton SO17 1BJ, UK
- <sup>2</sup>Optoelectronics Research Centre, University of Southampton, Southampton SO17 1BJ, UK

https://doi.org/10.1016/j.device.2025.100805

THE BIGGER PICTURE Neuromorphic computing uses electronic devices akin to biological synapses and neurons as building blocks in computing architectures. These architectures can emulate synaptic plasticity, supporting advanced learning and processing tasks in artificial intelligence (AI) hardware. Optoelectronic artificial synapses can simultaneously process electrical and optical signals, providing a promising pathway toward energy-efficient, high-performance neuromorphic systems. The technology has the potential to reduce the energy consumption down to femtojoules, enable multi-wavelength-sensitive visual processing, and simulate intricate neurological processes. In this perspective, we highlight how two-dimensional (2D) transition metal dichalcogenide (TMDC) materials can help advance these optoelectronic synaptic devices. 2D TMDCs have a layered structure that allows their electronic and optical properties to be tuned by controlling the number of layers, which enables tailored band gap and band alignment with other 2D materials and enhanced charge transport while providing mechanical flexibility useful for applications such as wearable devices.

### **SUMMARY**

Two-dimensional layered transition metal dichalcogenides (2D TMDCs), such as tungsten disulfide, molybdenum disulfide, compounds based on rhenium, and their heterostructures, have been used to fabricate artificial synaptic devices that combine memory, computation, and sensing in a single system. By using a combination of optoelectronic/electronic signal processing systems, these devices have demonstrated multi-state memory, pattern-recognition capabilities, biological synaptic behavior, and visual information processing. Their advanced scalability and integration potential render them ideal candidates for emerging neuromorphic memories in edge AI and wearable devices. Although ultra-low energy consumption in neuromorphic vision systems in the range of femtojoules has been achieved, optimizing the materials' quality and controlling the defect formation are still required to enhance their functionality and improve the devices' performance. Improving the scalability of heterostructures and integrating many single devices in arrays operating as part of a neuromorphic system are paramount to their commercialization.

### **INTRODUCTION**

Two-dimensional (2D) transition metal dichalcogenides (TMDCs) and their heterostructures have attracted attention in the emerging area of neuromorphic computing, due to their intriguing optoelectronic properties stemming from their low dimensionality. Light perception and cognition is an important sensory function for bioinspired electronics, for example, in artificial vision systems. The ability of 2D TMDC materials to combine electrical with optical operations enables development of synthetic retinas as well as optoelectronic interfaces for integrated photonic circuits.

Optoelectronic artificial synapses co-locate the optical signal-detection and memory functions in a single unit, thus being capable of sensing and memorizing information, giving rise to humanoid optoelectronic devices. Compared to purely electrical artificial synapses, optoelectronic ones involve a noncontact writing method and could enhance the processing speed because of their high bandwidth and ultrafast signal transmission, critical for low-power computation in edge-Al applications. Moreover, low crosstalk can be obtained, owing to the photo-writing being orthogonal to the electrical readout, providing a spatially confined stimulation

<sup>\*</sup>Correspondence: d.georgiadou@soton.ac.uk





that can offer secure authentication in decentralized devices, like biometric systems.  $^{3,4}$ 

In this perspective, we discuss the optoelectronic synaptic devices, which are enabled by the strong light-matter coupling in 2D TMDC. These materials possess a highly tunable band gap, which covers from visible to infrared, and undergo a direct-to-indirect band-gap transition when increasing the number of layers from monolayer to bulk.<sup>5</sup> The various energy-band configurations that can be designed by engineering van der Waals (vdW) homo- or heterostructures<sup>6</sup> open new avenues to the development of optoelectronic/electronic synaptic and heterosynaptic devices. As an example, monolayers with <1-nm thickness of MoS<sub>2</sub>, MoSe<sub>2</sub>, and WS<sub>2</sub> can absorb up to 5%–10% incident sunlight, which represents more than 10-fold increase in sunlight absorption compared with GaAs and Si, the common materials used in solar cells.<sup>7</sup>

Next, we summarize some key optical properties of the main TMDC materials that are being used in optoelectronic synaptic applications. Then, we explore how these materials have been incorporated in optoelectronic neuromorphic applications. We focus on two-terminal devices, which we believe are advantageous to transistors in terms of higher integration into dense crossbar arrays, simpler fabrication, and faster switching speed. The extra degree of freedom for programming and controlling neuromorphic operation that is provided by the gate terminal in mem-transistors is replaced by an optical source (acting as the gate) in the optoelectronic two-terminal devices. We introduce the operating mechanism and transport phenomena in TMDC-based optoelectronic memristive devices and then we showcase representative examples of emerging applications realized with single-layer TMDC and TMDC heterostructures, comprising either different TMDC or a TMDC material and an oxide layer.

### TRANSITION METAL DICHALCOGENIDE MATERIALS CONSIDERATIONS

TMDCs are layered materials with stoichiometry MX<sub>2</sub>, where M is a transition metal atom and X is a chalcogen. The transition metals encountered in TMDCs usually belong to groups IVB (titanium, Ti; zirconium, Zr; hafnium, Hf), VB (vanadium, V; niobium, Nb; tantalum, Ta), VIB (molybdenum, Mo; tungsten, W), VIIB (technetium, Tc; rhenium, Re), and VIIIB (palladium, Pd; platinum, Pt), while the most commonly employed chalcogen elements from group VIA are sulfur (S), selenium (Se), and tellurium (Te) (see Figure 1A).8 TMDC thin films are composed of a layer of metal atoms sandwiched between two atomic layers of the chalcogen. The atoms in the MX<sub>2</sub> structure are covalently bonded and the layers are stacked together by weak vdW bonds. The transition metal atom contributes four electrons to bond with chalcogen atoms, resulting in oxidation states of +4 for the transition metal and -2 for the chalcogen atom. MX<sub>2</sub> monolayers can exist in three phases, namely 1T, 2H, and 3R, where numbers represent the number of layers in the unit cell and the letters T, H, and R indicate trigonal prismatic, hexagonal, and rhombohedral symmetry, respectively (examples shown in Figure 1B). The structural phase transitions that can be achieved between these polymorphs can give rise to a multitude of reliable and fast switching states, similar to those induced by ion migration in resistive random-access memories (RRAMs) and by amorphous-to-crystalline transitions encountered in phase-change materials (PCMs).

Tungsten disulfide (WS<sub>2</sub>) is a well-known TMDC material with intriguing optoelectronic properties that involve high optical absorption coefficient (in a broad-spectrum region from visible to the near infrared [NIR]), high carrier mobility, high aspect ratio, and excellent thermal and chemical stability. The band gaps of bulk and monolayer WS<sub>2</sub> are 1.3 eV (indirect) and 2.1 eV (direct), respectively. The energy band of WS<sub>2</sub> shows a noticeable split in the valence band at the K point caused by the spin-orbit coupling. This leads to a strong photoluminescence and a large light-absorption coefficient.

Another critical material used in optoelectronic applications is molybdenum disulfide (MoS<sub>2</sub>), which has a unique crystal structure consisting of covalently bonded molybdenum and sulfur atoms, with layers spaced apart by approximately 6.5 Å and held together by vdW forces.  $^{15}$  MoS<sub>2</sub> exhibits a tunable band gap, approximately 1.2 eV for bulk and 1.8 eV for monolayer, as well as high carrier mobility.  $^{16}$  Molybdenum diselenide (MoSe<sub>2</sub>) has a 1.1 eV indirect band gap in bulk films and 1.5 eV direct band gap in its monolayer structure, slightly smaller than MoS<sub>2</sub> due to the effect of the chalcogen (Se) atom p<sub>z</sub> orbital in the valence band maxima.  $^{17}$  Similar to WS<sub>2</sub>, MoS<sub>2</sub>, and MoSe<sub>2</sub>, the bandgap of MoTe<sub>2</sub> can also be tuned, although at smaller scale (1.0 and 1.1 eV for bulk and single layer, respectively).  $^{18}$ 

Rhenium-based materials, such as rhenium disulfide (ReS<sub>2</sub>) and rhenium diselenide (ReSe<sub>2</sub>), exhibit slightly different properties, owing to their weaker interlayer coupling. ReS<sub>2</sub> maintains the characteristics of a direct-band-gap semiconductor across different layer numbers, showing stable optical properties and a bandgap of around 1.5–1.6 eV.<sup>19</sup> Similarly, ReSe<sub>2</sub>, which is of isoelectronic nature with ReS<sub>2</sub>, shows potential for further tuning of magnetic and optical properties via strain engineering due to its lattice distortion, while its bandgap is weakly layer dependent and decreases from 1.31 eV for thin layers to 1.29 eV in thick flakes.<sup>20</sup> The stability of the optical properties with increasing number of layers gives these materials a technological advantage over other 2D materials, as a monolayer is not required for a direct bandgap.<sup>21</sup>

### TMDC OPTOELECTRONIC NEUROMORPHIC APPLICATIONS

### Operating mechanisms of TMDC-based optoelectronic devices

Optoelectronic synaptic devices that integrate both optical and electrical stimulation to process and store information have opened a new outlook in neuromorphic computing. The key components of an optoelectronic synaptic device involve input stimulation, signal detection and processing, synaptic weighting, and signal output. The input stimulation can be electrical (current or voltage) and/or optical signals. The use of optical signal as the input stimulus offers major benefits, such as low power consumption, minimal signal interference (low crosstalk), and high bandwidth, and it avoids delay caused by resistance





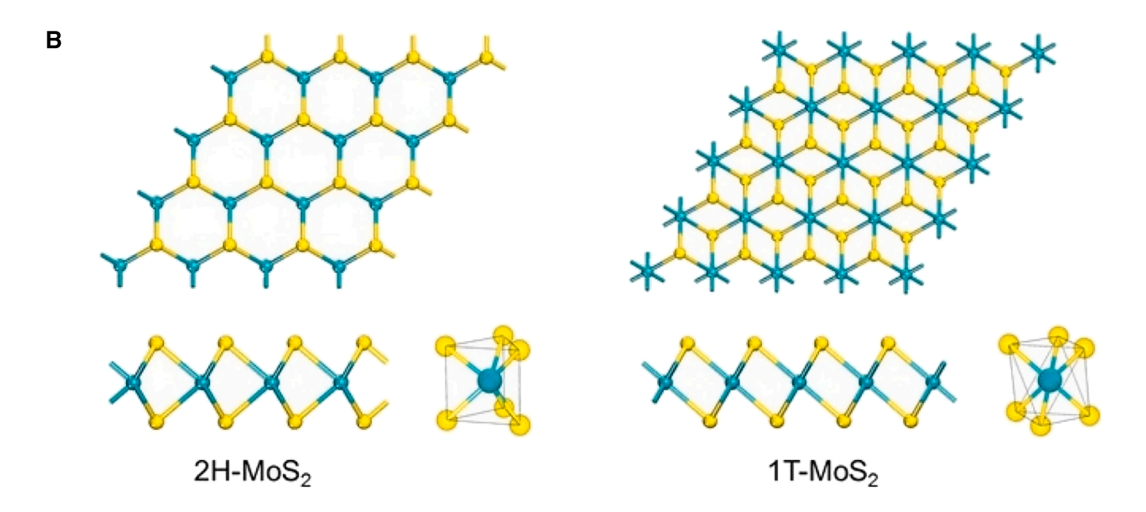


Figure 1. Transition metal dichalcogenide materials and their monolayer structures

(A) Periodic table of the known experimentally synthesized layered transition metal dichalcogenide materials with a summary of their existing structural phases (H, trigonal prismatic; T, octahedral; T', distorted octahedral; T<sub>d</sub>, orthorhombic), typical band gaps (values at the bottom left corner of each grid; M, metallic), and observed electronic phases (superconducting, topological, and charge density wave [CDW]). Adapted from Xue et al. <sup>10</sup>
(B) 2H trigonal prismatic and 1T octahedral coordination of metal atoms in the unit cell of MoS<sub>2</sub> monolayer structure. <sup>11</sup>

capacitance (RC), which are common pitfalls encountered in purely electrical inputs.<sup>4</sup>

There are various mechanisms responsible for the operation of a synaptic device, such as creation of conductive filaments, phase change, vacancy migration, and charge trapping/de-trapping.<sup>1</sup> Especially for an optoelectronic device that couples the optical and electrical stimulation to achieve the synaptic functionalities, photo-induced doping<sup>22</sup> and trapping/de-trapping<sup>23</sup> of photogenerated charge carriers at the interfaces or defect sites are the main mechanisms responsible for the switching





and for mimicking synaptic behaviors. By inducing trap sites in a TMDC, we can modify its conductivity, which is analogous to the modification of the synaptic weight.

Shallow trap levels are created by substitutional defects and are located around 10 meV of the valence or conduction band.<sup>24</sup> They enhance charge-carrier mobility and result in fast switching speeds. On the contrary, deep traps, created from vacancies, span a range of 0.1–0.4 eV inside the band gap and are responsible for hysteresis, charge storage, and long-term memory effects, as the optical information can be "remembered" by the retention of these trapped carriers even after the stimulus has been removed.<sup>25</sup> Grain boundaries are impeding charge transport and serve as a spatial barrier where the vacancies accumulate, influencing the size and location of conducting-filament formation in 2D memristive devices. By engineering the several types of defects in TMDCs during synthesis or upon applying some type of post-treatment, one can control many of the properties that define the synaptic plasticity of the devices and their short- and long-term memories.

Interface-induced trap states occur near the semiconductor-dielectric boundary due to imperfections like structural irregularities or impurities, impacting the optoelectronic behavior of devices by trapping carriers at the interface, and are often regulated through electric double layers (EDLs). Heterojunction-induced trap states arise in heterostructures, including vdW interfaces between different 2D materials, which are designed to improve charge separation, control charge trapping in specific layers, and optimize carrier transport via engineered band alignment.

Together, these mechanisms allow optoelectronic synaptic devices to couple optical and electrical signals, achieving complex synaptic functionalities and paving the way for advancements in neuromorphic computing and Al hardware.

### Single-layer optoelectronic synaptic devices

A memristive device is a two-terminal non-volatile memory device capable of remembering its resistance state induced by voltage or current applied to it, even after the original stimulus has been removed. The concept of the memristor (i.e., memory resistor) was proposed by Chua in 1971,26 and the first memristive device was demonstrated in 2008.<sup>27</sup> Such a device typically consists of three layers (two metal electrodes and a storage layer). The storage layer can be reconfigured by stimulating with either electrical or optical signals and can lead to memory effects. Recently, by controlling the volatility characteristics of a memristive device, it was found that both neuronal and synaptic behaviors can be emulated.<sup>28</sup> Therefore, memristive devices are leading candidates for future neuromorphic computing systems by offering on-chip reconfigurable memory with highdensity integration.<sup>29</sup> The optoelectronic memristive device integrates optical and electronic stimuli to achieve advanced dataprocessing and memory capabilities that can closely mimic biological neural networks. Retinomorphic devices can perform image-recognition tasks and be used in vision systems with ultra-low power consumption, while other neuronal functionalities, such as visual nociception, can be also emulated. We have selected some representative examples from recent literature to position 2D TMDC materials at the forefront of this technology.

### Retinomorphic devices and arrays

The retinomorphic devices mimic the way the retina processes the visual information. The retina captures the light signals via photoreceptor cells, called rods and cones, and the visual data are pre-processed through neural layers before transmitting them to brain via the optic nerve, 30 as shown in Figure 2A. Recent advancements have demonstrated the potential of WS2 to be employed in retinomorphic devices compatible with machinelearning algorithms toward hardware-based artificial neural networks (ANNs). For instance, a 2D WS2 retinomorphic memristive array was developed as part of an in-sensor reservoir computing system to facilitate the recognition and classification of traffic signals.<sup>30</sup> The WS<sub>2</sub> memristive device (Figure 2B) demonstrated excellent optoelectronic synaptic properties, including excitatory post-synaptic current (EPSC), paired-pulse facilitation (PPF), short-term potentiation (STP), and long-term potentiation (LTP) characteristics, which are shown in Figures 2C-2F. With this system, the handwritten numbers could be recognized with an accuracy of 88.3%, and 100% recognition rate for traffic signals of (red-green-blue) RGB wavelengths was achieved.

### Image recognition

Taking advantage of the WS $_2$  capability for broadband light sensing, optoelectronic resistive memory devices performing image-recognition tasks were fabricated. The broad wavelength range from 360 to 950 nm serves as the optical stimulus, with the device being highly responsive to 950 nm at room temperature. Both electrical and optical stimuli were applied to control the set/reset behavior of the WS $_2$  memristor. Potentiation and depression were achieved by applying 32 optical (2 s, 90  $\mu$ W cm $^{-2}$ ) and electrical pulses (2 s, -10 V), respectively. The WS $_2$  photonic synapses were used to recognize images from the Modified National Institute of Standards and Technology (MNIST) datasets and obtained an accuracy of 98.27%, showcasing the high potential of this material for integrated sensing and computing-memory functionalities.

More "exotic" devices, such as the "memitter" (memory emitter), have been enabled by a monolayer WS2, showing synaptic plasticity and visual memory characteristics. 32 A memitter device is an all-optical neuromorphic type of data-processing system that utilizes the adaptive photoluminescent (PL) (instead of the adaptive resistance that typically occurs in memristors) response of WS2 monolayer when exposed to optical stimulation. When WS<sub>2</sub> was exposed to continuous-wave 520-nm laser irradiation, the PL intensity increased over time due to the reduction in the n-doping of WS2 resulting from electron transfer to the laser-induced adsorption of atmospheric molecules like O<sub>2</sub> and H<sub>2</sub>O, and it decreased gradually after removing the laser light stimulus or after applying engineered pulsed optical waves. The device demonstrated the memorization and forgetting process that mimics biological synaptic behavior upon monitoring the change in photoluminescence emission intensity. The WS<sub>2</sub> memitter performed short-term synaptic behavior and spatialprocessing capabilities that render it suitable for storing the visual information. It supports pattern recognition and fading memory effects, akin to visual short-term memory (VSTM) of human brain, and can serve as a platform for physical-reservoir computing. The capability of the 2D memitter to sense, process, and memorize/forget optical inputs in the same physical



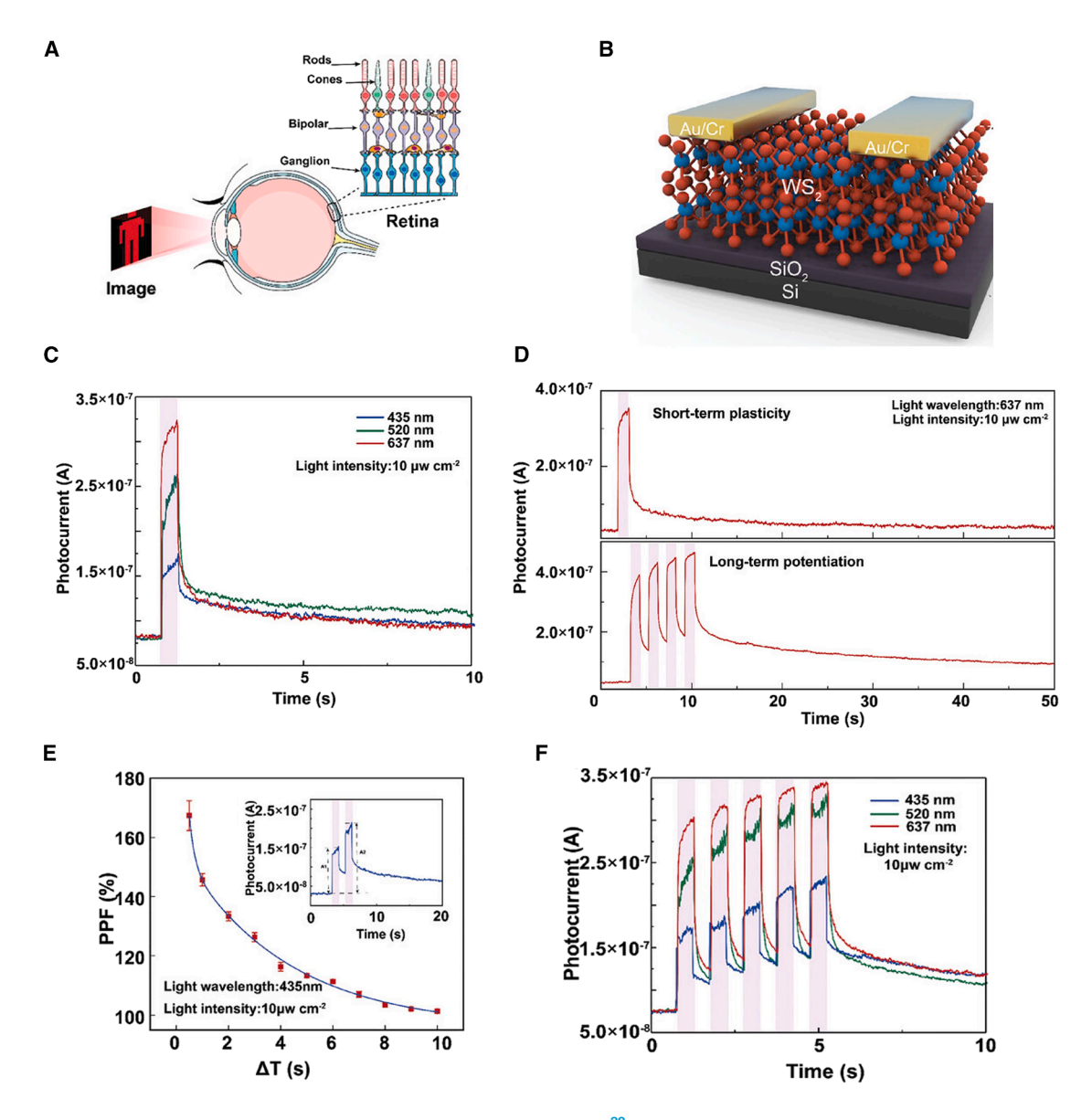


Figure 2. Synaptic functionalities of a retinomorphic WS<sub>2</sub> memristive device<sup>30</sup>

- (A) Schematic illustration of human vision system.
- (B) Schematic of  $WS_2$  retinomorphic memristive device.
- (C) EPSC response induced by RGB light stimuli.
- (D) Short- and long-term plasticity (potentiation) behavior of WS<sub>2</sub> memristive device upon illumination with 637-nm wavelength pulses.
- (E) Variation in paired-pulse facilitation (PPF) with different pulse intervals.
- (F) Long-term potentiation characteristics observed for different wavelengths of light.

substrate can be utilized for in-sensor computing. The incorporation of an in-sensor system could overcome the hardware bottleneck of using separate sensors and processors.

Optoelectronic operation of memristive devices can be further combined with other 2D TMDC material properties, such as ferroelectricity, for increased performance in image-recognition tasks. In a report by Yan et al., the fabricated ReSe<sub>2</sub> ferroelectric memristor with structure Pd/Al<sub>2</sub>O<sub>3</sub>/ReSe<sub>2</sub>/SiO<sub>2</sub>/Si was stimulated by both all-optical and electrical signals.<sup>33</sup> When the device is electrically or optically triggered, it switches between

the high resistive state (HRS) and low resistive state (LRS) owing to the change in the barrier height at the  $Al_2O_3$  and  $SiO_2$  interfaces with the  $ReSe_2$  caused by polarization flipping in the ferroelectric 2D material. The device shows long-term potentiation and depression under illumination with visible light, although the linearities of the weight update (i.e., conductance change) were 0.94 and 0.88 for potentiation and depression, respectively, which was lower than the ones achieved for electrical-only input pulses (0.99 and 0.98). This high linearity resulted in an error rate of 2.96% when the  $ReSe_2$  ferroelectric synapses





data were inserted in a training and inference simulation algorithm, implementing a six-layer convolutional neural network (CNN) using handwritten digit datasets from the MNIST database for image recognition. For reference, the error rate of digital recognition based on the ideal synaptic CNN was 1.15%.

### Neuromorphic vision system with ultra-low power consumption

One of the grand challenges that novel materials and device structures promise to address is the lowering of the power consumption of incumbent (Si-based) neuromorphic chips to the level of biological-equivalent systems. To this end, Chen et al. fabricated an ReS2-based optoelectronic synaptic memristor for a neuromorphic vision system (NVS) with ultra-low energy consumption of about 12.2 fJ.34 Unlike traditional vision systems, which mainly handle 2D images, their device enables 3D object recognition (stereo vision) by the fusion of its planar and depth images. The latter is formed by a conductance matrix that is based on distance detection due to different scattering of light from an object placed at various distances, which results in conductance changes. The ReS2-based NVS device shows high recognition rate of 97.05% for 3D objects, when simulated using data from the optoelectronic ReS2 synapses, and low-accuracy recognition rate of 32.6% for 2D objects without the synapses inserted in the same network structure. These devices with stereo-vision-like capabilities are suitable for applications requiring secure verification and prevention of 2D spoofing, such as face recognition and entrance guard systems.

### Visual nociceptor

Along the lines of developing artificial neural systems akin to the biological eye and the image-processing capabilities in the brain, nociception is another interesting concept that researchers attempted to emulate by designing intelligent electronic devices. Visual nociceptors are essential sensory neurons that send the pain signals to the visual cortex of the brain for processing. This mechanism is responsible for protecting humans from potential harm when dangerous environmental stimuli, such as intense light, exceed a certain threshold. Replicating these pain-sensing behaviors is crucial for emulating the advanced bionic vision systems in a simple design that integrates both sensing and processing into a single device. Wavelength-sensitive pain detection is also important for minimizing potential harm and improving the design of bionic vision systems. The intensity threshold for light causing retinal damage decreases for shorter wavelengths. If the eye has been already exposed/damaged by shorter wavelength, even the harmless longer-wavelength light can lead to secondary damage.

A monolayer MoS<sub>2</sub> was employed to fabricate a wavelength-sensitive artificial nociceptor that integrates both sensing and processing capabilities.<sup>35</sup> The optical synaptic device demonstrates persistent photoconductivity (PPC) upon illumination, owing to the existence of dangling bonds and charged impurities at the MoS<sub>2</sub>/SiO<sub>2</sub> interface, which allows emulation of synaptic functions, such as PPF, STP-to-LTP transitions, and memorizing/forgetting behaviors. The device also exhibits the wavelength-sensitive visual nociceptor functions, such as threshold detection, no adaptation to harmful stimulus and relaxation, as well as allodynia and hyperalgesia, which are shown in Figure 3.

Due to the PPC effect, the longer the optical pulse and the greater its intensity, the higher the photocurrent produced, as more electron-hole pairs are generated; therefore, the nociceptor threshold is crossed (akin to the feeling of pain in humans). This threshold is, however, wavelength dependent, as the absorptance of the material is not constant across the whole visible spectrum but, same as the human eye, the damage is higher (i.e., the threshold is reached at lower intensities) when exposed to shorter wavelengths (for the same amount of time).

#### **TMDC-based heterostructure devices**

The simple fabrication of devices comprising a single semiconducting layer of a 2D TMDC material, using minimum process steps, has obvious advantages, which is why most reports so far include these structures. However, heterostructures comprising at least one 2D TMDC, albeit more challenging to fabricate, as they require extra steps for the heterostructure assembly and alignment, provide access to new properties and applications beyond their single components' characteristics. These heterostructures offer multifunctionality and can respond to multi-wavelength illumination, due to tailoring of their optical properties through band-gap engineering.

More specifically, vdW heterostructures consist of stacked 2D materials integrated with 1D, 2D, or 3D bulk materials held together by weak vdW forces. These structures feature atomically sharp interfaces, minimal lattice mismatch, and tunable optical and electronic properties. The absence of dangling bonds at the interfaces minimizes defect-induced scattering and recombination and enhances the properties of optoelectronic devices. The in-plane migration of intrinsic defects that occurs in heterosynaptic connections is very attractive for realistically emulating biological neural networks.

TMDC materials can form heterostructures with other TMDCs or with semiconducting metal oxides. A MoS<sub>2</sub>/cerium oxide (CeO<sub>2</sub>) heterojunction was demonstrated that integrates a multifunctional artificial visual system with electrical storage, light sensing and memory, and visual nociceptors.<sup>39</sup> The authors demonstrated both electric- and light-induced synaptic plasticity. The change in conductance variation was studied and a  $9 \times 9$  memristor array was used to sense and memorize images with the aid of a UV-light stimulus with voltage-assisted modulation. In addition, a 7 × 7 optoelectronic memristor array was used to emulate the human vision for traffic signal, using multiwavelength optical modulation (620, 580, and 520 nm), while they also demonstrated visual nociceptors. The features of biological nociceptor, such as threshold, no adaptation, relaxation, and sensitization, were realized. CeO2 exhibits strong absorption in the UV band, but the presence of oxygen defects and excitation of electrons into the conduction band under the photoelectric effect contribute to its photo-response at visible wavelengths.

By taking advantage of the distinct optical properties of both materials, an MoS<sub>2</sub>/zinc oxide (ZnO) heterostructure was employed in multi-wavelength sensing and memory.<sup>40</sup> This heterostructure device can sense UV, blue, green, and red light by using the oxygen dissociation of annealed ZnO (UV- and visible-light environment) and the persistent photoconductivity effect of MoS<sub>2</sub> in the visible light. The device senses and memorizes UV



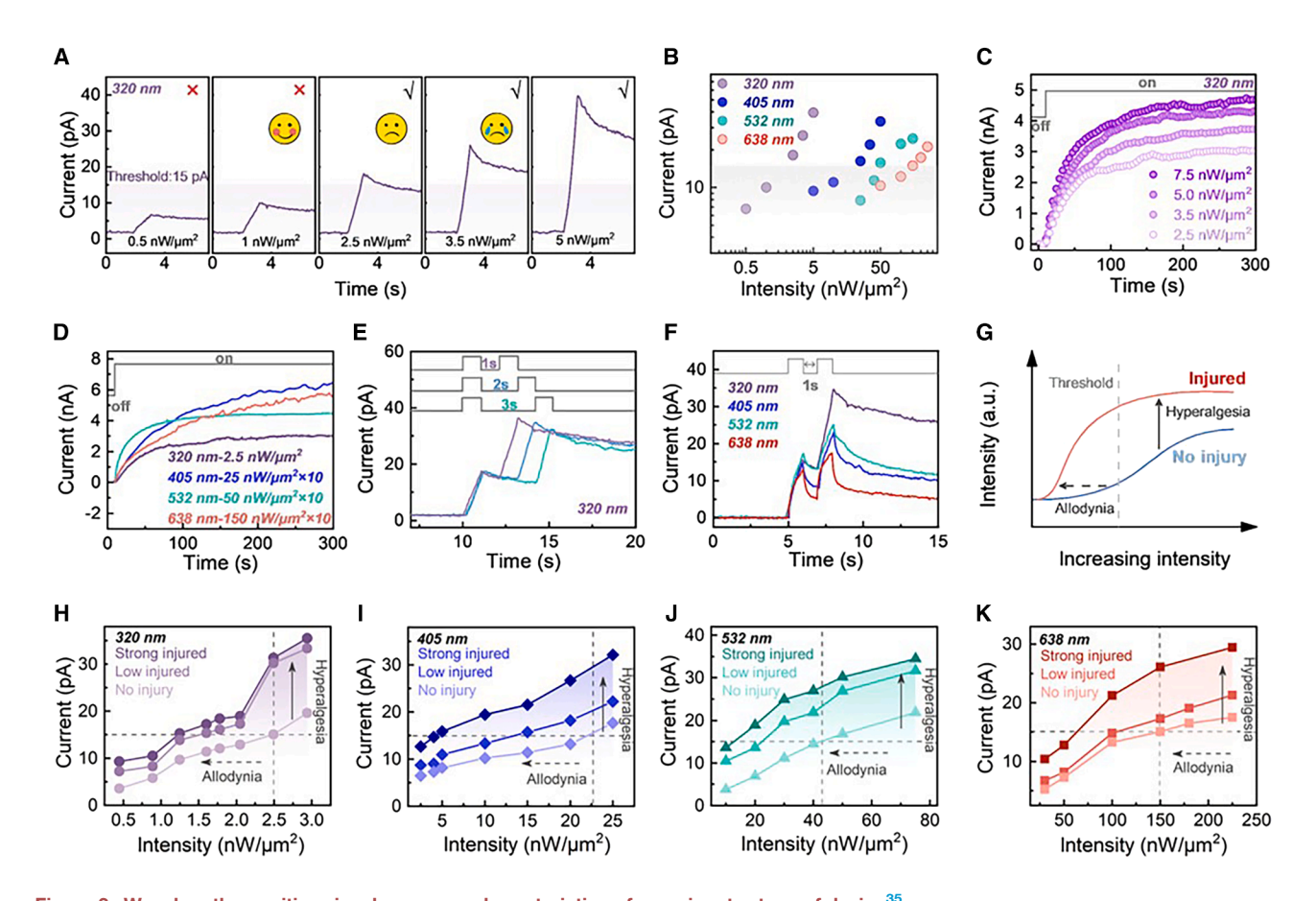


Figure 3. Wavelength-sensitive visual response characteristics of a nociceptor type of device<sup>35</sup>
(A) The device exhibits photocurrent responses at 320 nm under varying light intensities, showing a clear threshold behavior.
(B) The device's threshold response varies depending on the wavelength of the incident light, showcasing its wavelength sensitivity.

(C and D) (C) No-adaptation behavior of device at different intensity levels, and (D) different wavelengths.

(E and F) (E) The device demonstrates relaxation responses with varying time intervals between the pulses and (F) with varying wavelength.

(G–K) (G) Illustration of allodynia (pain from non-painful stimuli) and hyperalgesia (increased sensitivity to pain) with varying stimulus intensity and (H–K) wavelength-sensitive pain responses. The device mimics hyperalgesia and allodynia at different wavelengths.

light due to photogenerated carriers and changes in depletion region due to oxygen dissociation. For visible light, sensing and memory are enabled by trap states in  $MoS_2$  and increased oxygen vacancies in ZnO nanowires upon annealing. The basic synaptic functions, such as EPSC, PPF, STP, and LTP, were achieved, and the device could also emulate a wavelength-sensitive nociceptor.

Most TMDC materials are n-type semiconductors, the same as the majority of metal oxides; therefore, heterojunctions like the ones mentioned above cannot form p-n junctions that are suitable for efficient photodetection, as is the case of in-memory light-sensing applications. To this end, Li et al. fabricated a phosphorus (P)-doped MoSe<sub>2</sub>/phosphorous oxide (P<sub>x</sub>O<sub>y</sub>) heterostructure by depositing partially oxidized black phosphorus (BP) on Mo and controllably selenizing it. The resulting bilayer of p-type P-MoSe<sub>2</sub> and n-type P<sub>x</sub>O<sub>y</sub> formed a p-n junction that was used for efficient separation of photogenerated electronhole pairs. When light with wavelength 470–655 nm was shone on the heterojunction, the presence of the oxygen vacancies and photogenerated carriers contributed to the modulation of

conductance, which is a key factor in the synaptic behavior of the memristor.

vdW heterostructures comprising two distinct 2D TMDCs can deliver higher performance than their single counterparts. For example, an ReS<sub>2</sub>/WS<sub>2</sub>-based planar memristive device showed a higher switching ratio of 10<sup>6</sup> than the single ReS<sub>2</sub> memristive devices, better endurance and retention, and higher integration density.42 The resistive switching in the memristive device occurs due to the formation of conducting filaments by sulfur (S) vacancies. The ReS<sub>2</sub> layer generates more S vacancies due to their lower stoichiometric ratio than WS2. Therefore, the resistive switching is more dominant in the ReS<sub>2</sub> layer, while the WS<sub>2</sub> layer maintains the HRS. The heterostructure memristive device emulated the biological synapses, with S vacancies acting as the neurotransmitters in biological synapses, and voltage pulses acting as the stimulus signals. Because of the interlayer coupling and charge transfer of ReS2/WS2 heterostructure, it exhibits photoresponsive behavior; therefore, this structure can emulate optoelectronic memristor characteristics as well. The conductance level changed with the optical power density, showing



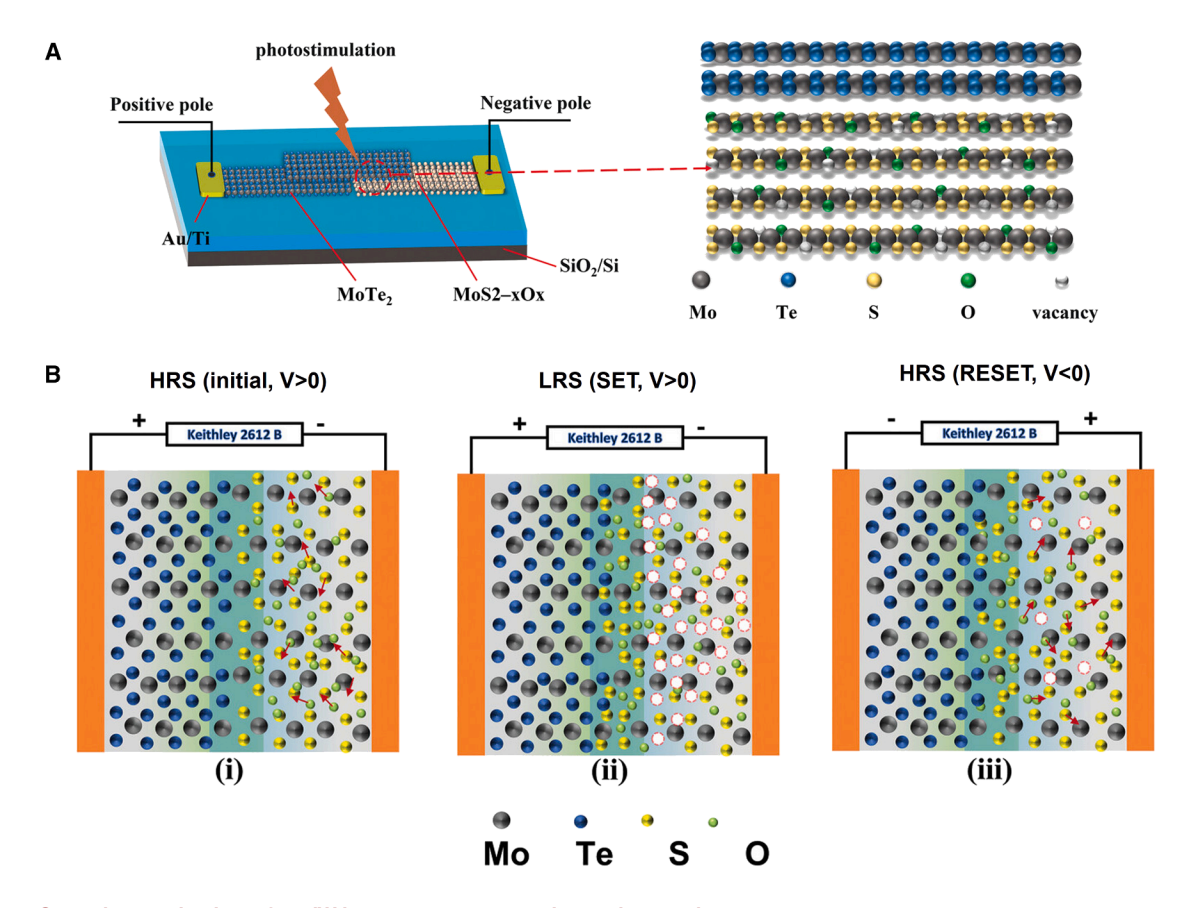


Figure 4. Operating mechanism of a vdW heterostructure optoelectronic memristor

(A) Illustration of the structure of an  $MoTe_2/MoS_{2-x}O_x$  memristor operating in optical and electronic mode and zoomed-in region of the molecular structure of a vertical heterostructure stack.

(B) Resistive switching mechanism of MoTe<sub>2</sub>/MoS<sub>2-x</sub>O<sub>x</sub> memristors. (i) Distribution of the atoms of the elements within the heterostructured device in the initial state and the migration trends of oxygen and sulfur ions under positive bias toward the positive electrode. (ii) Ion aggregation in the heterojunction stacking region under forward bias and the appearance of oxygen vacancies and sulfur vacancies in the MoTe<sub>2</sub>/MoS<sub>2-x</sub>O<sub>x</sub> interface region forming a conducting filament (LRS, SET). (iii) Ion migration toward the opposite direction and vacancy filling under negative bias (HRS, RESET).

Adapted from Xiao et al.<sup>43</sup>

the optical tunability of synaptic weight under 532-nm light stimulus. This kind of structure can be implemented in future visual neural applications.

The interfaces of 2D TMDC heterostructures can be engineered to comprise defects that enhance the optoelectronic properties of memristive synaptic devices. For instance, by exposing the MoS2 layer to UV ozone, Mo-O bonds are formed, and these lattice defects in the MoS2-xOx can be utilized to facilitate ion migration in MoTe<sub>2</sub>/MoS<sub>2-x</sub>O<sub>x</sub> vdW heterostructures (Figure 4A).43 This heterostructure leverages the domain-lifting effect of oxygen ion defect states in MoS<sub>2-x</sub>O<sub>x</sub> and narrow absorption band gap of MoTe2 to enhance the carrier transport (Figure 4B). The short- and long-term depression and potentiation were achieved shining the visible (532 nm) and NIR (1,064 nm) laser on top of the MoS<sub>2-x</sub>O<sub>x</sub> and MoTe<sub>2</sub>, respectively. A high accuracy rate of 99.3% was achieved for the electronic synapses and of 96.5% for the photonic synapses in recognizing MNIST handwritten digits, while the accuracy was lower for recognition of flower images, namely 95.3% and 91.5%, respectively. The improved accuracy of the electrical synapses is attributed to the higher linearity of their conducting states.

Another interesting approach is to merge optical response with other functionalities that can enable multimodal sensing in future intelligent electronic devices. Hou et al. fabricated an MoS<sub>2</sub>/WSe<sub>2</sub> vdW heterojunction to replicate artificial visual synapses by utilizing the photoconductivity (current response caused by light) and pyroconductivity (current response caused by temperature rise) mechanism. 44 The vdW heterojunction exhibits broadband synaptic behavior from visible to infrared region (405-1,064 nm) with low power consumption of 0.3-1.1 pJ per spike. The MoS<sub>2</sub>/WSe<sub>2</sub> vdW heterojunction has lower power consumption than the single-layer MoS2 and WSe2 devices, as the built-in field at the heterointerface results in lower dark current, which in turn improves the optical detection performance. Additionally, the pyroconductivity observed in the MoS<sub>2</sub>/WSe<sub>2</sub> vdW heterojunction improved the synaptic performance, as it stabilizes the post-synaptic current created after illumination for a longer time after the light is turned off, as the temperature does not return to room temperature instantly.



Material	Synthesis of TMDC	Wavelength (nm)	PPF (%)	Energy consumption (nJ)	Accuracy rate (%)	Reference
A. Single-TMDC-la	yer devices					
WS <sub>2</sub>	exfoliation	435 520 637	~170 - -	5 12 18	100	Gong et al. <sup>30</sup>
WS <sub>2</sub>	sulfurization	950	_	_	98.27	Sharmila et al.31
1L WS2	CVD	520	102	-	-	Ferrarese Lupi et al.32
1L MoS <sub>2</sub>	mechanical exfoliation	320 405 532 638	57.8	-	-	Li et al. <sup>35</sup>
MoS <sub>2</sub>	CVD	532	∼116	-	-	Sathyanarayana and Das <sup>46</sup>
ReS <sub>2</sub>	mechanical exfoliation	450-805	124	$1.212 \times 10^{-5}$	97.0	Chen et al. <sup>34</sup>
ReSe <sub>2</sub>	solid-phase sintering and spin coating	405 520 650	-	-	97.4	Wang et al. <sup>33</sup>
B. Heterostructures	3					
CeO <sub>2</sub> /MoS <sub>2</sub>	hydrothermal	UV 520 580 620	25	-	-	Lin et al. <sup>39</sup>
P-MoSe <sub>2</sub> /P <sub>x</sub> O <sub>y</sub>	selenization	470 590 655 808	3.35 2.58	-		Li et al. <sup>41</sup>
MoS <sub>2</sub> /ZnO	mechanical exfoliation	375 490 525 625 800	149 159 164	2.55	-	Li et al. <sup>40</sup>
MoTe <sub>2</sub> /MoS <sub>2-x</sub> O <sub>x</sub>	mechanical exfoliation	532-1,064	_	_	95.3	Xiao et al.43
MoS <sub>2</sub> /WSe <sub>2</sub>	mechanical exfoliation	660 1,064 1,550	- 66.7 41.8	$3 \times 10^{-4}$ 1. 1 × 10 <sup>-3</sup> 4 × 10 <sup>-4</sup>	-	Qiu et al. <sup>44</sup>
ReS <sub>2</sub> /WS <sub>2</sub>	CVD	532 690	-	-	-	Huang et al. <sup>42</sup>

### **CONCLUSIONS AND OUTLOOK**

Inspired by the biological neural network, optoelectronic synaptic devices are opening new horizons in neuromorphic computing. 2D transition metal dichalcogenides and their heterostructures are potential candidates for optoelectronic synaptic devices because of their unique physical and chemical properties, such as layered structure and bandgap tunability, strong light-matter interaction, high carrier mobility and switching speed, broad spectral response, and energy efficiency. The atomically thin nature of these 2D materials provides an advantage for low operation voltage and ultra-low energy consumption (Table 1) as well as mechanical flexibility, attributes that are paramount in edge-Al wearable devices, like smart lenses and artificial retinas to treat vision impairment or employed in robotics. For example, the Young's modulus (E) of monolayer MoS2 is 25% that of graphene  $(E_{MoS2} = 240 \text{ GPa}, E_{graphene} = 1 \text{ TPa})$ , while their shearstrength values are comparable (100–200 GPa).<sup>45</sup> Despite the optical properties being slightly dependent on strain, this does not define their performance, and it can be engineered to strengthen the optoelectronic performance of TMDC-based flexible devices and systems.

Their scalability potential to enable nanometer devices, as demonstrated by Taiwan Semiconductor Manufacturing Company's (TSMC) monolayer MoS<sub>2</sub> nanosheet field-effect transistor with a gate length of 40 nm<sup>47</sup> and their complementary metal oxide semiconductor (CMOS) integration in large-area substrates, as shown by IMEC's high-quality growth of WS<sub>2</sub> on 300-mm wafers using a modified metal-organic chemical vapor deposition (MOCVD) method, <sup>48</sup> could further accelerate progress in the 2D neuromorphic memories. <sup>49</sup> However, as these are high-temperature processes, transfer of the 2D layer after growth or alternative low-temperature and low-cost chemical exfoliation methods need to be considered for use with flexible (temperature-sensitive) substrates. <sup>50</sup>





WS2, MoS2, WSe2, and their various heterostructures have been used for the past couple of years and have advanced from research experiments to potential solutions for Al hardware and machine vision. The 2D TMDC-based optoelectronic synaptic devices can emulate brain-like synaptic behavior and recognize patterns with extremely low energy consumption (fJ). Optoelectronic or fully optical control has been achieved, while wavelength sensitivity or broadband response can be obtained by choosing the suitable material from the wide range of existing layered transition metal dichalcogenides. Their rich optoelectronic properties allow the development of more exotic devices that can leverage their photoluminescence or ferroelectric characteristics. 51 Multimodal sensing is also possible, as showcased in the photo- and pyroconductivity study. The large surface/volume ratio of 2D TMDC materials permits the physical adsorption (i.e., physisorption) of interacting molecules on the TMDC surface via non-covalent interactions and electron-transfer processes that modify their resistance, rendering them suitable for electrochemical or gas sensing.52 This multifunctionality and versatility in external stimuli that can be employed to modify the devices' resistance is useful in in-sensor computing architectures that offer higher integration density and lower fabrication complexity. These attributes are desirable in flexible light-weight multimodal sensing systems for wearable neuromorphic systems that could replace injured nerves or study sensory and central nervous system disorders and for portable sensing devices for the Internet of Things (IoT).

However, there are challenges to overcome in order to reach higher performance, in terms of lower energy consumption (the biological analog imposes reaching <aJ levels on electronics), greater device stability, and higher degree of scalability that will enhance their commercialization potential. The material quality can be improved via optimized synthesis routes and additional post-synthesis treatments to control the defect formation, such as annealing, plasma etching, and chemical functionalization. More research focus should be placed on different types of heterostructures, such as 2D perovskites/TMDC, which present intriguing photophysics and band-engineering potential due to the tuneability of the organic spacer of the 2D perovskites. 53 Twistronics has emerged as a novel approach for 2D materials to tune their optical and electrical properties (e.g., dielectric constant, refractive index, extinction coefficient, absorption coefficient) by modifying the rotation angles in the superposition of the periodic structures of the TMDC on each other, providing further flexibility for using the same material in different applications.<sup>54</sup>

Additional device-engineering methods, such as surface treatments and contact engineering, can reduce the interlayer impurities and enhance the charge-transfer kinetics. Scaling up the heterostructures apart from the single layers and system integration of the synaptic device arrays for real-world use will help unlock their full potential for future neuromorphic and human vision systems that are expected to revolutionize future computing, robotics, and wearable electronics.

### **ACKNOWLEDGMENTS**

Both authors wish to acknowledge the support from the UKRI Future Leaders Fellowship Grant (MR/V024442/1). D.G.G. also acknowledges support from

European Union's HORIZON Europe Project TEAM-NANO under grant agreement no. 101136388.

#### **AUTHOR CONTRIBUTIONS**

R.S.B. wrote the first draft and was responsible for the initial literature research. D.G.G. conceived and coordinated the work; reviewed, revised, and edited the full text; and compiled the final version after revisions.

#### **DECLARATION OF INTERESTS**

The authors declare no competing interests.

#### REFERENCES

- Jana, R., Ghosh, S., Bhunia, R., and Chowdhury, A. (2024). Recent developments in the state-of-the-art optoelectronic synaptic devices based on 2D materials: a review. J. Mater. Chem. C Mater. 12, 5299–5338. https://doi.org/10.1039/D4TC00371C.
- Lee, Y., Oh, J.Y., Xu, W., Kim, O., Kim, T.R., Kang, J., Kim, Y., Son, D., Tok, J.B.-H., Park, M.J., et al. (2018). Stretchable organic optoelectronic sensorimotor synapse. Sci. Adv. 4, eaat7387. https://doi.org/10.1126/ sciadv.aat7387.
- He, H.-K., Yang, R., Zhou, W., Huang, H.-M., Xiong, J., Gan, L., Zhai, T.-Y., and Guo, X. (2018). Photonic Potentiation and Electric Habituation in Ultrathin Memristive Synapses Based on Monolayer MoS2. Small 14, 1800079. https://doi.org/10.1002/smll.201800079.
- Wang, J., Ilyas, N., Ren, Y., Ji, Y., Li, S., Li, C., Liu, F., Gu, D., and Ang, K.W. (2024). Technology and integration roadmap for optoelectronic memristor. Adv. Mater. 36, 2307393. https://doi.org/10.1002/adma.202307393.
- Sun, Y., Wang, D., and Shuai, Z. (2016). Indirect-to-Direct Band Gap Crossover in Few-Layer Transition Metal Dichalcogenides: A Theoretical Prediction. J. Phys. Chem. C 120, 21866–21870. https://doi.org/10.1021/ acs.jpcc.6b08748.
- Tian, M.-Y., Gao, Y.-M., Zhang, Y.-J., Ren, M.-X., Lv, X.-H., Hou, K.-X., Jin, C.-D., Zhang, H., Lian, R.-Q., Gong, P.-L., et al. (2024). Toward direct band gaps in typical 2D transition-metal dichalcogenides junctions via real and energy spaces tuning. Commun. Mater. 5, 188. https://doi.org/10.1038/ s43246-024-00631-z.
- Bernardi, M., Palummo, M., and Grossman, J.C. (2013). Extraordinary Sunlight Absorption and One Nanometer Thick Photovoltaics Using Two-Dimensional Monolayer Materials. Nano Lett. 13, 3664–3670. https://doi.org/10.1021/nl401544y.
- Tang, C.S., and Yin, X. (2024). Two-dimensional Transition Metal Dichalcogenides: A General Overview. In Two-Dimensional Transition-Metal Dichalcogenides, A. Wee, X. Yin, and C.S. Tang, eds., pp. 1–59. https://doi. org/10.1002/9783527838752.ch1.
- Sun, Y., Wang, S., Zhang, Q., and Zhou, P. (2024). Evaluation of different 2D memory technologies for in-memory computing. Device 2, 100509. https://doi.org/10.1016/j.device.2024.100509.
- Xue, G., Qin, B., Ma, C., Yin, P., Liu, C., and Liu, K. (2024). Large-Area Epitaxial Growth of Transition Metal Dichalcogenides. Chem. Rev. 124, 9785–9865. https://doi.org/10.1021/acs.chemrev.3c00851.
- Jadhav, J., Waghadkar, Y., Padwal, Y., Hashem, M., Fouad, H., Kekade, S. S., Terashima, C., Chauhan, R., Charhate, S., Gosavi, S.W., and Late, D.J. (2024). Enhanced dye degradation using 2H-MoS2 and 1T@2H-MoS2: A comparative study. J. Solid State Electrochem. https://doi.org/10.1007/s10008-024-05813-w.
- Li, C., Sang, D., Ge, S., Zou, L., and Wang, Q. (2024). Recent Excellent Optoelectronic Applications Based on Two-Dimensional WS2 Nanomaterials: A Review. Molecules 29, 3341. https://doi.org/10.3390/molecules 29143341.
- Lin, L., Xu, Y., Zhang, S., Ross, I.M., Ong, A.C.M., and Allwood, D.A. (2013). Fabrication of luminescent monolayered tungsten dichalcogenides



- quantum dots with giant spin-valley coupling. ACS Nano 7, 8214–8223. https://doi.org/10.1021/nn403682r.
- Ernandes, C., Khalil, L., Henck, H., Zhao, M.-Q., Chaste, J., Oehler, F., Johnson, A.T.C., Asensio, M.C., Pierucci, D., Pala, M., et al. (2021). Strain and spin-orbit coupling engineering in twisted WS2/graphene heterobilayer. Nanomaterials 11, 2921. https://doi.org/10.3390/nano11112921.
- Zou, L.-R., Sang, D.-D., Yao, Y., Wang, X.-T., Zheng, Y.-Y., Wang, N.-Z., Wang, C., and Wang, Q.-L. (2023). Research progress of optoelectronic devices based on two-dimensional MoS2 materials. Rare Met. 42, 17–38. https://doi.org/10.1007/s12598-022-02113-y.
- Wang, H., Li, C., Fang, P., Zhang, Z., and Zhang, J.Z. (2018). Synthesis, properties, and optoelectronic applications of two-dimensional MoS 2 and MoS 2-based heterostructures. Chem. Soc. Rev. 47, 6101–6127. https://doi.org/10.1039/C8CS00314A.
- Mahatha, S.K., Patel, K.D., and Menon, K.S.R. (2012). Electronic structure investigation of MoS2 and MoSe2 using angle-resolved photoemission spectroscopy and ab initio band structure studies. J. Phys. Condens. Matter 24, 475504. https://doi.org/10.1088/0953-8984/24/47/475504.
- Yamamoto, M., Wang, S.T., Ni, M., Lin, Y.-F., Li, S.-L., Aikawa, S., Jian, W.-B., Ueno, K., Wakabayashi, K., and Tsukagoshi, K. (2014). Strong Enhancement of Raman Scattering from a Bulk-Inactive Vibrational Mode in Few-Layer MoTe2. ACS Nano 8, 3895–3903. https://doi.org/10.1021/nn5007607.
- Tongay, S., Sahin, H., Ko, C., Luce, A., Fan, W., Liu, K., Zhou, J., Huang, Y.-S., Ho, C.-H., Yan, J., et al. (2014). Monolayer behaviour in bulk ReS2 due to electronic and vibrational decoupling. Nat. Commun. 5, 3252. https://doi.org/10.1038/ncomms4252.
- Jariwala, B., Voiry, D., Jindal, A., Chalke, B.A., Bapat, R., Thamizhavel, A., Chhowalla, M., Deshmukh, M., and Bhattacharya, A. (2016). Synthesis and Characterization of ReS2 and ReSe2 Layered Chalcogenide Single Crystals. Chem. Mater. 28, 3352–3359. https://doi.org/10.1021/acs.chemmater.6b00364.
- Rahman, M., Davey, K., and Qiao, S.-Z. (2017). Advent of 2D Rhenium Disulfide (ReS2): Fundamentals to Applications. Adv. Funct. Mater. 27, 1606129. https://doi.org/10.1002/adfm.201606129.
- Xu, M., Xu, T., Yu, A., Wang, H., Wang, H., Zubair, M., Luo, M., Shan, C., Guo, X., Wang, F., et al. (2021). Optoelectronic synapses based on photoinduced doping in MoS2/h-BN field-effect transistors. Adv. Opt. Mater. 9, 2100937. https://doi.org/10.1002/adom.202100937.
- Islam, M.M., Dev, D., Krishnaprasad, A., Tetard, L., and Roy, T. (2020). Optoelectronic synapse using monolayer MoS2 field effect transistors. Sci. Rep. 10, 21870. https://doi.org/10.1038/s41598-020-78767-4.
- Huang, P., Lukin, R., Faleev, M., Kazeev, N., Al-Maeeni, A.R., Andreeva, D. V., Ustyuzhanin, A., Tormasov, A., Castro Neto, A.H., and Novoselov, K.S. (2023). Unveiling the complex structure-property correlation of defects in 2D materials based on high throughput datasets. npj 2D Mater. Appl. 7, 6. https://doi.org/10.1038/s41699-023-00369-1.
- Jiang, J., Xu, T., Lu, J., Sun, L., and Ni, Z. (2019). Defect Engineering in 2D Materials: Precise Manipulation and Improved Functionalities. Research 2019, 4641739. https://doi.org/10.34133/2019/4641739.
- Chua, L. (1971). Memristor-the missing circuit element. IEEE Trans. Circuit Theory 18, 507–519. https://doi.org/10.1109/TCT.1971.1083337.
- Strukov, D.B., Snider, G.S., Stewart, D.R., and Williams, R.S. (2008). The missing memristor found. Nature 453, 80–83. https://doi.org/10.1038/ nature06932.
- Woo, K.S., Park, H., Ghenzi, N., Talin, A.A., Jeong, T., Choi, J.-H., Oh, S., Jang, Y.H., Han, J., Williams, R.S., et al. (2024). Memristors with Tunable Volatility for Reconfigurable Neuromorphic Computing. ACS Nano 18, 17007–17017. https://doi.org/10.1021/acsnano.4c03238.
- Zidan, M.A., Strachan, J.P., and Lu, W.D. (2018). The future of electronics based on memristive systems. Nat. Electron. 1, 22–29. https://doi.org/10. 1038/s41928-017-0006-8.

- Gong, Y., Xing, X., Wang, X., Duan, R., Han, S.T., and Tay, B.K. (2024). Integrated Bionic Human Retina Process and In-Sensor RC System Based on 2D Retinomorphic Memristor Array. Adv. Funct. Mater. 34, 2406547. https://doi.org/10.1002/adfm.202406547.
- Sharmila, B., and Dwivedi, P. (2024). Wafer scale WS2 based ultrafast photosensing and memory computing devices for neuromorphic computing. Nanotechnology 35, 425201. https://doi.org/10.1088/1361-6528/ad6006.
- Ferrarese Lupi, F., Milano, G., Angelini, A., Rosero-Realpe, M., Torre, B., Kozma, E., Martella, C., and Grazianetti, C. (2024). Synaptic Plasticity and Visual Memory in a Neuromorphic 2D Memitter Based on WS2 Monolayers. Adv. Funct. Mater. 34, 2403158. https://doi.org/10.1002/adfm.20 2403158.
- Wang, H., Yang, J., Wang, Z., Shao, Y., Tang, Y., Guo, J., and Yan, X. (2024). Reconfigurable multifunctional neuromorphic memristor fabricated from two-dimensional ReSe2 ferroelectric nanosheet films. Appl. Phys. Rev. 11, 011402. https://doi.org/10.1063/5.0170147.
- Chen, Y., Huang, Y., Zeng, J., Kang, Y., Tan, Y., Xie, X., Wei, B., Li, C., Fang, L., and Jiang, T. (2023). Energy-efficient ReS2-based optoelectronic synapse for 3D object reconstruction and recognition. ACS Appl. Mater. Interfaces 15, 58631–58642. https://doi.org/10.1021/acsami.3c14958.
- Li, J., Zhou, Y., Li, Y., Yan, C., Zhao, X.-G., Xin, W., Xie, X., Liu, W., Xu, H., and Liu, Y. (2024). Perceiving the Spectrum of Pain: Wavelength-Sensitive Visual Nociceptive Behaviors in Monolayer MoS2-Based Optical Synaptic Devices. ACS Photonics 11, 4578–4587. https://doi.org/10.1021/acsphotonics.4c00877
- Novoselov, K.S., Mishchenko, A., Carvalho, A., and Castro Neto, A.H. (2016). 2D materials and van der Waals heterostructures. Science 353, aac9439. https://doi.org/10.1126/science.aac9439.
- Liao, W., Huang, Y., Wang, H., and Zhang, H. (2019). Van der Waals heterostructures for optoelectronics: Progress and prospects. Appl. Mater. Today 16, 435–455. https://doi.org/10.1016/j.apmt.2019.07.004.
- Ryu, Y.K., Frisenda, R., and Castellanos-Gomez, A. (2019). Superlattices based on van der Waals 2D materials. Chem. Commun. 55, 11498– 11510. https://doi.org/10.1039/C9CC04919C.
- Lin, Y., Wang, W., Li, R., Kim, J., Zhang, C., Kan, H., and Li, Y. (2024). Multifunctional optoelectronic memristor based on CeO2/MoS2 heterojunction for advanced artificial synapses and bionic visual system with nociceptive sensing. Nano Energy 121, 109267. https://doi.org/10.1016/j.nanoen. 2024.109267.
- Li, Z., Zou, G., Xiao, Y., Feng, B., Huo, J., Peng, J., Sun, T., and Liu, L. (2024). MoS2/ZnO-heterostructured optoelectronic synapse for multiwavelength optical information-based sensing, memory, and processing. Nano Energy 127, 109733. https://doi.org/10.1016/j.nanoen.2024.109733.
- Li, Y., Sun, H., Yue, L., Yang, F., Dong, X., Chen, J., Zhang, X., Chen, J., Zhao, Y., Chen, K., and Li, Y. (2024). Multicolor Fully Light-Modulated Artificial Synapse Based on P-MoSe2/PxOy Heterostructured Memristor. J. Phys. Chem. Lett. 15, 8752–8758. https://doi.org/10.1021/acs.jpclett. 4c01980.
- Huang, F., Ke, C., Li, J., Chen, L., Yin, J., Li, X., Wu, Z., Zhang, C., Xu, F., Wu, Y., and Kang, J. (2023). Controllable resistive switching in ReS2/WS2 heterostructure for nonvolatile memory and synaptic simulation. Adv. Sci. 10, 2302813. https://doi.org/10.1002/advs.202302813.
- Xiao, Y., Li, W., Lin, X., Ji, Y., Chen, Z., Jiang, Y., Liu, Q., Tang, X., and Liang, Q. (2023). 2D MoTe2/MoS2-xOx Van der Waals heterostructure for bimodal neuromorphic optoelectronic computing. Adv. Electron. Mater. 9, 2300388. https://doi.org/10.1002/aelm.202300388.
- Qiu, D., Zheng, S., and Hou, P. (2024). Simulating and Implementing Broadband van der Waals Artificial Visual Synapses Based on Photoconductivity and Pyroconductivity Mechanisms. ACS Appl. Mater. Interfaces 16, 53142–53152. https://doi.org/10.1021/acsami.4c10128.
- Jiang, D., Liu, Z., Xiao, Z., Qian, Z., Sun, Y., Zeng, Z., and Wang, R. (2022).
   Flexible electronics based on 2D transition metal dichalcogenides. J. Mater.
   Chem. A Mater. 10, 89–121. https://doi.org/10.1039/D1TA06741A.

Please cite this article in press as: Babu and Georgiadou, 2D transition metal dichalcogenides for energy-efficient two-terminal optoelectronic synaptic devices, Device (2025), https://doi.org/10.1016/j.device.2025.100805





- 46. Sathyanarayana, S., and Das, B.C. (2024). Grain boundary effect unveiled in monolayer MoS 2 for photonic neuromorphic applications. J. Mater. Chem. C 12, 13827-13839. https://doi.org/10.1039/D4TC02912G.
- 47. Chung, Y.Y., Chou, B.J., Hsu, C.F., Yun, W.S., Li, M.Y., Su, S.K., Liao, Y.T., Lee, M.C., Huang, G.W., Liew, S.L., et al. (2022). First Demonstration of GAA Monolayer-MoS2 Nanosheet nFET with 410 $\mu$ A  $\mu$  m ID 1V VD at 40nm gate length. In 2022 International Electron Devices Meeting (IEDM) (IEEE), pp. 34.35.31-34.35.34. https://doi.org/10.1109/IEDM45625.2022. 10019563.
- 48. Huyghebaert, C., Schram, T., Smets, Q., Kumar Agarwal, T., Verreck, D., Brems, S., Phommahaxay, A., Chiappe, D., El Kazzi, S., Lockhart de la Rosa, C., et al. (2018). 2D materials: roadmap to CMOS integration. In 2018 IEEE International Electron Devices Meeting (IEDM) (IEEE), pp. 22.21.21-22.21.24. https://doi.org/10.1109/IEDM.2018.8614679.
- 49. Kim, S.J., Lee, H.-J., Lee, C.-H., and Jang, H.W. (2024). 2D materialsbased 3D integration for neuromorphic hardware. npj 2D Mater. Appl. 8, 70. https://doi.org/10.1038/s41699-024-00509-1.

- 50. Raza, A., Hassan, J.Z., Ikram, M., Ali, S., Farooq, U., Khan, Q., and Maqbool, M. (2021). Advances in Liquid-Phase and Intercalation Exfoliations of Transition Metal Dichalcogenides to Produce 2D Framework. Adv. Mater. Interfaces 8, 2002205. https://doi.org/10.1002/admi.202002205.
- 51. Chen, C., Zhou, Y., Tong, L., Pang, Y., and Xu, J. (2025). Emerging 2D Ferroelectric Devices for In-Sensor and In-Memory Computing. Adv. Mater. 37, 2400332. https://doi.org/10.1002/adma.202400332.
- 52. Hassan, J.Z., Raza, A., Din Babar, Z.U., Qumar, U., Kaner, N.T., and Cassinese, A. (2023). 2D material-based sensing devices: an update. J. Mater. Chem. A Mater. 11, 6016-6063. https://doi.org/10.1039/D2TA07653E.
- 53. Baranowski, M., Surrente, A., and Plochocka, P. (2022). Two Dimensional Perovskites/Transition Metal Dichalcogenides Heterostructures: Puzzles and Challenges. Isr. J. Chem. 62, e202100120. https://doi.org/10.1002/ ijch.202100120.
- 54. Gupta, N., Sachin, S., Kumari, P., Rani, S., and Ray, S.J. (2024). Twistronics in two-dimensional transition metal dichalcogenide (TMD)-based van der Waals interface. RSC Adv. 14, 2878-2888. https://doi.org/10. 1039/D3RA06559F.